

Brain Mitochondrial Drug Delivery: Influence of Drug Physicochemical Properties

Shelley A. Durazo · Rajendra S. Kadam · Derek Drechsel · Manisha Patel · Uday B. Kompella

Received: 31 May 2011 / Accepted: 29 June 2011 / Published online: 28 July 2011
© Springer Science+Business Media, LLC 2011

ABSTRACT

Purpose To determine the influence of drug physicochemical properties on brain mitochondrial delivery of 20 drugs at physiological pH.

Methods The delivery of 8 cationic drugs (beta-blockers), 6 neutral drugs (corticosteroids), and 6 anionic drugs (non-steroidal anti-inflammatory drugs, NSAIDs) to isolated rat brain mitochondria was determined with and without membrane depolarization. Multiple linear regression was used to determine whether lipophilicity (Log D), charge, polarizability, polar surface area (PSA), and molecular weight influence mitochondrial delivery.

Results The Log D for beta-blockers, corticosteroids, and NSAIDs was in the range of -1.41 to 1.37 , 0.72 to 2.97 , and -0.98 to 2 , respectively. The % mitochondrial uptake increased exponentially with an increase in Log D for each class of drugs, with the uptake at a given lipophilicity obeying the rank order cationic > anionic > neutral. Valinomycin reduced membrane potential and the delivery of positively charged propranolol and betaxolol. The best equation for the combined data set was $\text{Log \% Uptake} = 0.333 \text{ Log D} + 0.157 \text{ Charge} - 0.887 \text{ Log PSA} + 2.032$ ($R^2 = 0.738$).

Conclusions Drug lipophilicity, charge, and polar surface area and membrane potential influence mitochondrial drug delivery, with the uptake of positively charged, lipophilic molecules being the most efficient.

KEY WORDS brain delivery · lipophilicity · membrane potential · mitochondrial delivery · polar surface area

ABBREVIATIONS

CNPase	2' 3'-cyclic nucleotide 3'-phosphodiesterase
EDTA	ethylenediaminetetraacetic acid
F	explained variance/unexplained variance
FL2/FL1	590 nm emission/525 nm emission
LC-MS/MS	liquid chromatography tandem mass spectrometry
LDH	lactate dehydrogenase
Log D	Log distribution coefficient
Log P	Log partition coefficient
MW	molecular weight
N	number of molecules
NSAIDs	non-steroidal anti-inflammatory drugs
PBS	phosphate-buffered saline
pKa	acid dissociation constant
PSA	polar surface area
Q	charge
R^2	amount of variance in dependent variable that is explained by model
SD	standard deviation
SE	standard error of the estimate
α	polarizability

Electronic Supplementary Material The online version of this article (doi:10.1007/s11095-011-0532-4) contains supplementary material, which is available to authorized users.

S. A. Durazo · R. S. Kadam · D. Drechsel · M. Patel ·
U. B. Kompella (✉)
Department of Pharmaceutical Sciences
University of Colorado Denver
12850 E. Montview Blvd.
Aurora, Colorado 80045, USA
e-mail: uday.kompella@ucdenver.edu

INTRODUCTION

Mitochondrial dysfunction underlies the pathology of various neurodegenerative diseases including Alzheimer's (1), Parkinson's (2), retinitis pigmentosa (3,4), and age-related macular degeneration (5). In several of these diseases, reactive oxygen species have been implicated as

important mediators. Thus, development and design of mitochondrial therapeutics, including targeted anti-oxidants and other agents, have become a major focus in treating the above diseases.

Several investigators have designed mitochondria-targeted therapeutics including small molecule and peptide compounds. Primea *et al.* designed S-nitrosothiols with positive charge and lipophilic groups in order to target mitochondria (6). Zhao *et al.* designed mitochondria-specific peptides by alternating aromatic residues with positively charged residues to inhibit mitochondrial swelling, cell death and reperfusion injury (7). Further, a mitochondria-targeted cationic plastoquinone (SkQ1) prevents oxidative damage and development of retinopathy and cataract in OXYS rats suffering from oxidative stress (8). Although there is general recognition that cationic, lipophilic molecules exhibit preferential mitochondrial delivery, there were no systematic reports investigating the influence of drug physicochemical properties on mitochondrial uptake of drugs belonging to various classes. Further, an earlier analysis of literature based on studies with isolated mitochondria and intact cells of various sources indicated that positive, neutral, as well as negatively charged molecules exhibit mitochondriotropic behavior or accessibility to mitochondria (9). Further, this previous analysis suggested that lipophilicity and cationic nature may not be essential requirements for mitochondrial delivery. In order to further test the influence of drug properties including charge on mitochondrial delivery in a single system, eight beta-blockers (positively charged), six corticosteroids (neutral), and six non-steroidal anti-inflammatory drugs (NSAIDs, negatively charged) were assessed as model drugs in this study. Drug uptake was measured in isolated brain mitochondria, and the % uptake was correlated to drug physicochemical properties including Log D, charge, polar surface area, polarizability, and molecular weight.

The potential difference of the inner mitochondrial membrane is maintained at approximately -240 mV (10) by the electron transport chain processes, which generate a proton gradient from inside the mitochondrial matrix towards the inter-membrane space to fuel the production of ATP and oxidation of NADH to NAD^+ . Based on high negative potential, it can be envisioned that positively charged compounds might undergo a charge gradient-driven enhancement in uptake, whereas neutral and negatively charged compounds do not. The importance of the membrane potential on the uptake of a variety of drugs was not thoroughly investigated in previous reports. Towards this end, we investigated mitochondrial delivery of the above positive, neutral, and negatively charged compounds in the presence and absence of valinomycin, a potassium ionophore, which allows influx of positively charged potassium ions into mitochondria, thereby depolarizing mitochondrial membrane potential.

MATERIALS AND METHODS

Materials

The following drugs from each class were obtained from Sigma-Aldrich (St. Louis, MO). Beta-blockers: propranolol HCl, betaxolol HCl, pindolol, nadolol, timolol maleate salt, metoprolol-tartrate salt, sotalol HCl and atenolol; corticosteroids: budesonide, flucinolone acetonide, triamcinolone acetonide, dexamethasone, prednisolone and triamcinolone; and NSAIDs: mefenamic acid, flurbiprofen, naproxen, ketoprofen, indoprofen and tolmetin sodium salt. Corticosterone, labetalol HCl, diclofenac sodium salt, valinomycin, and JC-1 dye were also obtained as solids from Sigma-Aldrich (St. Louis, MO). All solvents used were of HPLC grade.

Drug Physicochemical Properties and Log D Estimation

Physicochemical properties of beta-blockers, corticosteroids, and NSAIDs including Log MW, Log P (Log partition coefficient), pKa, polarizability (α), and polar surface area (PSA) were obtained using ACD/PhysChem Suite (version 12, ACD/Labs, Toronto, Canada). Mono-basic pKa values were obtained for beta-blockers, and monoacidic pKa values were obtained for corticosteroids and NSAIDs. Log D (distribution coefficient) values for beta-blockers and corticosteroids at pH 7.4 were obtained from previous studies in our laboratory (11,12). Log D values for NSAIDs (mefenamic acid, flurbiprofen, naproxen, ketoprofen, indoprofen and tolmetin) were measured using a shake flask technique in this study. The buffer (PBS, pH 7.4) and *n*-octanol were mutually saturated by shaking at 37°C for 12 h on a shaker incubator set at 300 rpm. Since mitochondrial uptake studies employed a cassette dosing approach, Log D was measured using NSAID cocktails prepared at two different concentrations (5 and 1.25 $\mu\text{g}/\text{ml}$ for each molecule) in PBS (pH 7.4) buffer. The distribution coefficient was determined by incubating 1 ml of NSAID buffer solution with 1 ml of *n*-octanol at 37°C for 24 h, while shaking at 300 rpm to reach distribution equilibrium. After 24 h, the two phases were separated (*n*-octanol and buffer) by centrifuging at 13,000 g for 10 min. The amount of drug in each phase was measured using an LC-MS/MS analysis. The Log D at pH 7.4 was calculated using the following equation: $\text{Log D} = \text{Log}(C_{\text{octanol}}/C_{\text{buffer}})$, where C_{octanol} and C_{buffer} refer to the concentration of drug in the *n*-octanol and buffer phase, respectively. Percent ionized at pH 7.4 was calculated for acids using the following equation: $\% \text{ ionized} = 100/(1 + \text{antilog}(\text{pKa} - 7.4))$. % ionized at pH 7.4 for the bases was calculated using the following equation: $\% \text{ ionized} = 100/(1 + \text{antilog}(7.4 -$

pKa)). Estimation of percent ionized was calculated using the monobasic pKa for beta-blockers and the monoacidic pKa for NSAIDs and corticosteroids.

Isolation of Mitochondria

Previously reported protocols were used for mitochondria isolation from rat brain, an organ rich in mitochondria (13–15). All animal procedures were conducted in accordance with the guidelines of the Institutional Animal Care and Use Committee (IACUC) at the University of Colorado Denver. Briefly, intact brain was excised from male Sprague Dawley rats after euthanizing the animals with CO₂ asphyxiation followed by decapitation. The brain was homogenized in an isolation buffer and subjected to Percoll™ density gradient centrifugation techniques to separate the mitochondria from cellular debris. The isolation buffer consisted of 0.32 M sucrose, 1 mM EDTA, and 10 mM Tris Base. The final mitochondrial pellet obtained after isolation was resuspended in respiration buffer (25 mM sucrose, 50 mM EDTA, 10 mM Tris Base, 75 mM mannitol, 100 mM KCl, 10 mM malate, and 2.5 mM glutamate) suitable for maintaining the integrity and function of the mitochondria. Mitochondrial protein concentration was determined using a bicinchoninic acid assay and a bovine serum albumin standard curve in the range of 1 to 0.0625 mg/ml.

Western Blot for Mitochondrial Purity

A 10-well 15–20% Tris Base Mini-Protean gel was purchased from Bio-Rad (Hercules, CA) for performing gel electrophoresis. Prior to loading samples into the sample wells, 3 µg of protein was mixed with 20 µl of loading dye and boiled for 3–4 min in a microwave. Electroporation was conducted at 25 mA for 80 min in the presence of running buffer (25 mM tris base, 192 mM glycine, 0.1% SDS). Protein transfer from the gel to the nitrocellulose membrane was conducted in a transfer apparatus at 100 mA for 3 h in the presence of transfer buffer (25 mM Tris Base, 192 mM glycine, 20% v/v methanol, pH 8.3). After transfer, the nitrocellulose membrane was washed 3 times in TBS-T buffer (20 mM tris HCl, 150 mM NaCl plus 1 ml of Tween-20, pH 8.3 in 1 L) for 5 min while shaking. Blocking was conducted in 5% (w/v) dried milk in TBS-T buffer for 2 h while shaking at room temperature. Three primary antibody solutions were used: 1) MitoProfile® Mitochondrial Integrity WB Antibody Cocktail (MS620, MitoSciences, Inc.), 2) lactate dehydrogenase (LDH) primary antibody (1173, Rockland, Inc.) and 3) 2', 3'-cyclic nucleotide 3'-phosphodiesterase (CNPase) primary antibody (2986, Cell Signaling Technology, Inc.) at 250, 2000, and 10,000 time dilutions, respectively. Primary antibody solutions were made in 5% milk in TBS-T and

incubated with the nitrocellulose membrane at 4°C for 16 h while shaking. Next, the membranes were washed 4 times for 10 min with TBS-T, and then the appropriate secondary antibodies were applied and incubated at room temperature while shaking for 1 h. The following horseradish peroxidase-labeled secondary antibodies were used: 1) anti-mouse for monoclonal MitoProfile antibody cocktail, 2) anti-goat for LDH antibody, and 3) anti-rabbit for CNPase antibody. Secondary antibodies were diluted 10,000 times in TBS-T. After incubating the membrane with the secondary antibodies, the membrane was washed 4 times in TBS-T for 5 min while shaking at room temperature. Bands were visualized by staining the membrane with an enhanced chemiluminescence kit (1:1 mixture of solution 1:2) and developing enhanced chemiluminescence film.

Measurement of Mitochondrial Membrane Potential

JC-1 dye is commonly used to detect relative strength of the mitochondrial membrane potential due to its ability to exist as a monomer at low mitochondrial membrane potential and as an aggregate at high mitochondrial membrane potential. When the membrane potential is weak (e.g., -20 mV), JC-1 emits strongly in the green region (525 nm), and when the membrane potential is extremely strong (e.g., -240 mV), JC-1 emits strongly in the red region (590 nm). Thus, JC-1 dye will emit strongly in the red region (590 nm) in normal mitochondria and in the green region (525 nm) when membrane potential is depolarized by an ionophore such as valinomycin, which is capable of depolarizing mitochondrial membrane potential by allowing entry of K⁺ ions. For the membrane potential experiments, a stock solution of 1 mg/ml JC-1 was made with 100% DMSO and diluted 5000 times to 0.2 µg/ml.

After pre-incubating mitochondria in respiration buffer containing 0.2 µg/ml JC-1 dye, various treatments were added to the samples. The treatments included buffer alone, buffer with 5 µM valinomycin, buffer with beta-blocker cassette (6.25 µg/ml each), buffer with corticosteroid cassette (0.3125 µg/ml each), and buffer with NSAID cassette (6.25 µg/ml each). The JC-1 dye was excited at 488 nm, and the fluorescence emission was recorded continuously every 2 min at 590 nm (FL2) and 525 nm (FL1) using the Spectromax M5 instrument and Softmax Pro 5.2 software at room temperature. FL2/FL1 ratio was estimated, and percent change in this parameter was used to monitor changes in the membrane potential difference (16).

Mitochondrial Uptake Studies

A cassette dosing approach was used to analyze the delivery of several compounds within three different drug classes

(beta-blockers, corticosteroids or non-steroidal anti-inflammatory drugs (NSAIDs)) to minimize mitochondrial usage and, consequently, animal use. Each class of drug has a different charge at physiological pH (pH=7.4): corticosteroids are neutral due to the absence of functional groups that can obtain a charge, beta-blockers are positively charged (pKa of approximately 9), and NSAIDs are negatively charged (pKa of approximately 4).

Each cassette stock and valinomycin stock was made in the respiration buffer. The concentrations of drug incubated with mitochondria were 5 µg/ml of beta-blockers and NSAIDs and 2.5 µg/ml corticosteroids. The volumes of drug, mitochondria, and treatment solutions were of equal volume for consistency: 200 µl of 6.25 µg/ml of beta-blockers and NSAIDs and 200 µl of 3.125 µg/ml corticosteroids; 37.5 µl of 8 mg/ml mitochondrial protein; 12.5 µl of 100 µM valinomycin or plain respiration buffer. Mitochondrial solutions containing drug were gently shaken at 37°C for 1 h to allow for uptake. After 1 h, uptake was terminated by centrifugation at 30,966 g at 4°C for 10 min. The pelleted mitochondria were washed with respiration buffer to remove any drug bound to the surface of the mitochondria and centrifuged again at 30,966 g at 4°C for 10 min to collect the supernatant for drug quantification. The pelleted mitochondria were resuspended with 200 µl of the internal standard in the mobile phase to extract the drug. Drug in extract was quantified using liquid chromatography and triple quadrupole mass spectroscopy (LC-MS/MS).

LC-MS/MS Analysis and Extraction Recovery

Samples from the mitochondrial uptake study were analyzed using simultaneous analysis method by liquid chromatography tandem mass spectrometry (LC-MS/MS). LC-MS/MS analysis was carried out using a Perkin-Elmer Model 200 HPLC system (Agilent Technologies, Palo Alto, CA) connected to an API-Sciex-3000 mass spectrometer. Separate LC-MS/MS methods were developed for each class of molecules and analyzed separately.

Beta-blocker quantification in both mitochondrial tissue and buffer samples were analyzed using a previously published method (17). Analyte separation was accomplished using Hypersil-ODS C18 column (100×2.1 mm, 3.5 µm) with gradient elution at a flow rate of 0.4 ml/min with a mobile phase containing 5 mM ammonium formate, pH 3.5 (A) and acetonitrile methanol (75:25 v/v) containing 0.02% triethyl amine, pH 3.5 (B). Briefly, the supernatant buffer and wash buffer samples of uptake study were diluted 5-fold with acetonitrile containing labetalol as an internal standard (250 ng/ml labetalol) to reduce the salt concentration and subjected to analysis. The mitochondrial tissue samples were processed using acetonitrile precipitation method and subjected to analysis. The analytes were

monitored in positive mode of ionization using the following transitions: 267/145 (atenolol); 273/255 (sotalol); 310/254 (nadolol); 249/116 (pindolol); 317/261 (timolol); 268/133 (metoprolol); 308/116 (betaxolol); 260/116 (propranolol); 327/162 (labetalol).

For corticosteroid uptake analysis, an analytical method previously developed by our laboratory was employed (12). Separation of analytes was carried out using a Sunfire C18 column (50×2.1 mm, 3.5 µm). The analytes were separated by gradient elution at a flow rate of 0.25 ml/min with the mobile phase containing 5 mM ammonium formate, pH 3.5 (A) and acetonitrile:methanol (50:50 v/v) (B). Corticosterone (250 ng/ml) was used as an internal standard during analysis. The supernatant and wash buffer samples were diluted 5-fold with acetonitrile, and mitochondrial samples were processed using acetonitrile protein precipitation method. The steroids were monitored in positive mode of ionization using the following transitions: 361/343 (prednisolone); 395/357 (triamcinolone); 393/373 (dexamethasone); 453/417 (flucinolone acetone); 435/415 (triamcinolone acetone); 431/413 (budesonide); 347/329 (corticosterone).

An LC-MS/MS method was developed in this study for measurement of NSAIDs. NSAIDs have a carboxyl group in their structure and, therefore, were analyzed in negative mode of ionization. Analyte separation was carried out using a Kromasil C18 column (50×2.1 mm, 3.5 µm) with the mobile phase containing water (A) and acetonitrile:methanol (50:50 v/v) (B). Analytes were eluted in gradient mode of elution at a flow rate of 0.25 ml/min, with a total run time of 7 min. The supernatant and wash buffer samples were diluted 5-fold with acetonitrile containing diclofenac as an internal standard (250 ng/ml diclofenac). Mitochondrial tissue samples were processed using an acetonitrile-based protein precipitation method whereby 200 µl of acetonitrile containing the internal standard was added to the pelleted mitochondria. Acetonitrile also facilitates drug extraction. The NSAIDs were monitored in negative mode of ionization using following transitions: 256/210 (tolmetin); 280/236 (indoprofen); 253/209 (ketoprofen); 229/185 (naproxen); 243/199 (flurbiprofen); 240/196 (mefenamic acid). Extraction recovery of the three cassettes was analyzed at 25, 250 and 1 µg/ml concentrations for each drug. The procedures were similar to the above sample analysis, whereby 200 µl of acetonitrile containing the internal standard and drug cassette was added to 50 µl of mitochondria preparation.

The extraction recovery was 86–153% for beta-blockers, 81–117% for corticosteroids, and 83–114% for NSAIDs.

Data Analysis and Model Construction

Mitochondrial drug uptake in 1 h was expressed as % dose uptake. Exponential correlations between percent uptake

and Log D as well as linear correlations between Log percent uptake and Log D were assessed for individual data sets (beta-blockers, corticosteroids, and NSAIDs) and the entire data set using Microsoft Excel 2010 (Redmond, WA). Further, using SPSS software (version 19, IBM, Armonk, NY), multiple linear regression was performed on three data sets: 1) mitochondrial uptake with strong membrane potential (absence of valinomycin), 2) mitochondrial uptake with dissipated membrane potential by valinomycin, and 3) differential mitochondrial uptake (difference in uptake between the absence and presence of valinomycin). For the various parameters of interest in predicting drug uptake of the combined data set, a correlation matrix was generated to identify parameters with collinearity. Parameters with a correlation coefficient (Pearson Correlation) greater than 0.5 were considered collinear. After reducing collinear parameters, linear regression was conducted on the combined data set as well as individual classes using enter and forward linear regression methods. The stepping method criteria for forward linear regression were determined using probability of F entry: 0.05 and removal: 0.1. Goodness of fit for model equations was determined by high R^2 , low P-value, low SE (standard error of the estimate), and high F value. Predictability and consistency of the best fit model equations were confirmed using a test set of 4 molecules (betaxolol, sotalol, dexamethasone, and indoprofen) randomly chosen using SPSS software, and the remaining 16 molecules were used as the training set. The predicted and actual values of mitochondrial uptake for the test set were correlated, and the R^2 values were determined. Statistical analysis was performed using two-tailed Student's *T*-test.

RESULTS

Drug Physicochemical Properties

Table I lists the names, structures, and physicochemical properties (MW, pKa, charge (Q) at pH 7.4, % ionized at pH 7.4, Log P (Log partition coefficient), Log D (Log distribution coefficient), Log α (polarizability), and Log PSA (polar surface area)) of each compound assessed in the mitochondrial uptake study. Log D measured for NSAIDs in this study ranged from -0.98 to 2 .

Identification of Mitochondrial Fraction

The method of mitochondrial isolation was scrutinized using a western blot to demonstrate purity of isolated mitochondria. The MitoProfile western blot in Fig. 1 clearly shows that mitochondrial proteins including cytochrome c, complex V (ATP synthase), cyclophilin D, and porin are present in isolated mitochondria as well as control

heart mitochondria. The purity was assessed by confirming the absence of two contaminant proteins in the mitochondrial fraction: 2', 3'-cyclic nucleotide 3'-phosphodiesterase (CNPase) and lactate dehydrogenase (LDH). CNPase is a neuronal protein found in myelin, and LDH is a cytosolic protein, also found in neuronal cells. These two contaminants were present in the whole brain homogenate, but absent in the isolated mitochondria and the control heart mitochondria (Fig. 1). These results demonstrate that the mitochondrial isolation method excludes contaminant proteins, CNPase and LDH. Thus, the mitochondrial preparation was free of neuronal and cytosolic contaminant proteins.

Valinomycin Dissipates the Mitochondrial Membrane Potential

Figure 2 shows changes in the membrane potential of mitochondria measured as FL2/FL1 ratio, in the presence of $5 \mu\text{M}$ valinomycin and each drug cassette. Valinomycin treatment rapidly decreased the FL2/FL1 ratio by about 50% in 1 h. Further, the decline in FL2/FL1 ratio was statistically different from control at 5 min ($p < 0.001$) and 1 h ($p < 0.001$). In comparison, drug treatment groups, corticosteroids and beta-blockers were not statistically different from control group immediately after addition or at 1 h and, hence, did not alter the membrane potential. NSAIDs reduced the FL2/FL1 ratio, which was not statistically significant immediately after addition ($p = 0.855$), but significantly lower at 1 h ($p = 0.005$), with the 1 h reduction being approximately 20%.

Mitochondrial Uptake is Influenced by Drug Physicochemical Properties

The positively charged beta-blockers exhibited higher uptake than negatively charged or neutral compounds at a given Log D, and within each class of molecules, the most lipophilic drug had the highest uptake (Fig. 3). For example, the positively charged drug betaxolol (Log D = 0.96) had 13% uptake, whereas neutral triamcinolone (Log D = 0.715) and negatively charged flurbiprofen (Log D = 0.92) of approximately the same Log D had only 3% ($p < 0.001$) and 6% ($p = 0.003$) uptake, respectively. In addition, budesonide (Log D = 2.98), a neutral compound, which is 2 times more lipophilic than the most lipophilic positively charged compound (propranolol, Log D = 1.4), had only 28% uptake compared to 44% for propranolol ($p = 0.004$). Thus, drug charge influences mitochondrial uptake of small molecules, with positively charged molecules being preferred. Negatively charged molecules exhibited intermediate uptake when compared to positively charged and neutrally charged molecules.

Table 1 Physicochemical Properties of Beta-Blockers, Corticosteroids, and NSAIDs Used in the Mitochondrial Uptake Study. Log P is the Log of the Partition Coefficient, Q Denotes Charge, α Denotes Polarizability, and PSA is Polar Surface Area. Log D (Log Distribution Coefficient) Measures for Beta-blockers and Corticosteroids were Obtained from Kadam et al. (11) and Thakur et al. (12), respectively. The Monobasic pKa Values are Reported for Beta-Blockers and Monoacidic pKa Values are Reported for Corticosteroids and NSAIDs. Log D Values for NSAIDs were Measured in this Study. Q, % Ionized, and Log D are Reported at pH 7.4

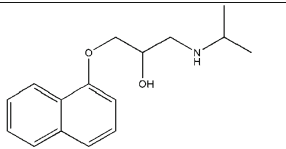
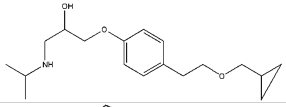
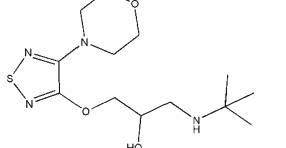
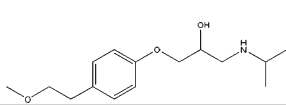
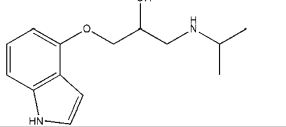
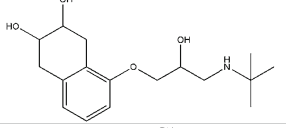
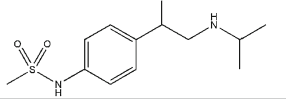
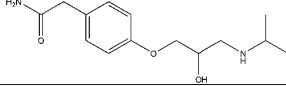
Drug	Chemical Structure	MW	pKa	Q	% Ionized _{7.4}	Log P	Log D _{7.4}	α (10^{-24}cm^3)	PSA (\AA^2)
Positively Charged (Beta-blockers)									
Propranolol		259.3	9.4	+1	99.4	2.9	1.37	31.31	41.5
Betaxolol		307.4	9.4	+1	99.4	2.53	0.96	35.25	50.7
Timolol		316.4	9.4	+1	99.0	1.28	0.35	32.57	108
Metoprolol		267.4	9.4	+1	99.6	1.63	0.2	30.55	50.7
Pindolol		248.3	9.5	+1	99.9	1.68	-0.1	29.11	57.3
Nadolol		260.0	9.5	+1	99.4	0.56	-1.06	33.99	82
Sotalol		272.4	9.3	+1	99.4	0.24	-1.21	28.6	86.8
Atenolol		266.3	9.4	+1	98.8	0.33	-1.41	29.44	84.6

Table 1 (continued)

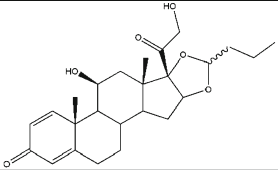
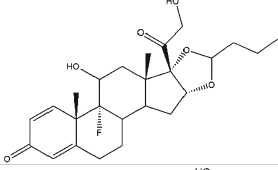
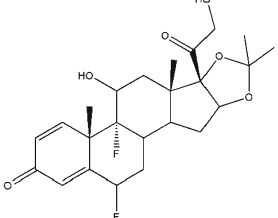
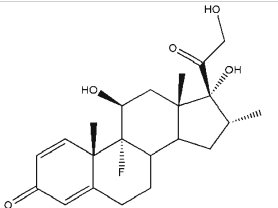
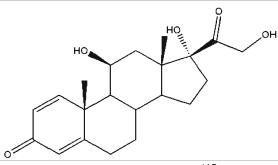
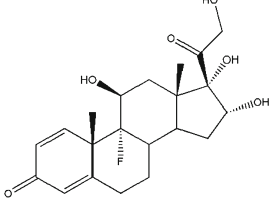
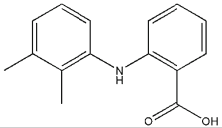
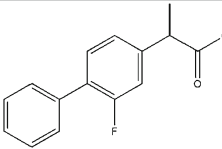
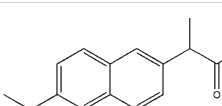
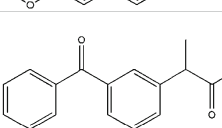
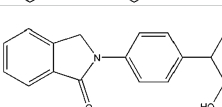
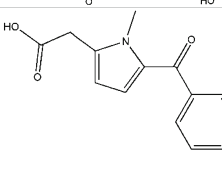
Drug	Chemical Structure	MW	pKa	Q	% Ionized _{7.4}	Log P	Log D _{7.4}	α (10^{-24}cm^3)	PSA (\AA^2)	
Neutral (Corticosteroids)										
Budesonide		430.5	12.9	0	0	3.2	2.97	45.14	93.1	
Triamcinolone Acetonide		434.5	12.9	0	0	3.07	2.58	45.2	93.1	
Fluocinolone Acetonide		452.5	12.8	0	0	2.23	2.56	43.41	93.1	
Dexamethasone		392.5	12.1	0	0	2.03	1.95	39.74	94.8	
Prednisolone		360.4	12.5	0	0	1.63	1.77	37.85	94.8	
Triamcinolone		394.4	11.6	0	0	0.53	0.715	38.51	115	

Table I (continued)

Drug	Chemical Structure	MW	pKa	Q	% Ionized _{7.4}	Log P	Log D _{7.4}	α (10^{-24}cm^3)	PSA (\AA^2)
Negatively Charged (NSAIDs)									
Mefenamic Acid		241.3	3.7	-1	100	4.83	2	28.63	49.3
Flurbiprofen		244.3	4.1	-1	99.9	3.66	0.92	26.4	37.3
Naproxen		230.3	4.8	-1	99.7	2.88	0.33	26.37	46.5
Ketoprofen		254.3	4.2	-1	99.9	2.91	-0.25	28.46	54.4
Indoprofen		281.3	4.4	-1	99.9	2.82	-0.38	30.81	57.6
Tolmetin		257.3	4.2	-1	99.9	2.68	-0.98	28.83	59.3

Valinomycin significantly reduced the uptake of propranolol ($p < 0.0001$) from 44% to 20% and betaxolol ($p = 0.034$) from 13% to 7%. Besides these effects on the most lipophilic positively charged compounds, valinomycin had no significant effect on the uptake of more hydrophilic positively charged compounds. In addition, valinomycin did not statistically alter the uptake of neutral or negatively charged compounds.

Within each class of molecules, lipophilicity or Log D influences mitochondrial uptake (Fig. 4). Based on Excel analysis, the Log % uptake of positively and neutrally charged compounds correlated significantly with Log D ($R^2 = 0.789$ and 0.888 , respectively), whereas the uptake of negatively charged compounds correlated less well with Log D ($R^2 = 0.519$). When all data were pooled together, the correlation between Log % uptake and Log D decreased ($R^2 = 0.646$) compared to positively and neutrally charged compounds and increased compared to negatively charged compounds. In exponential fits, the coefficient (4.61) and

the exponent ($e^{1.08\text{LogD}}$) were the highest for the % uptake of positively charged molecules, indicating their preferential uptake with an increase in Log D.

Mitochondrial Uptake Model Construction

We considered two parameters as colinear if the Pearson Correlation Coefficient was greater than 0.5 (Table II). Log P correlated with Log D (0.518), Q (-0.535) and Log PSA (-0.634). Log D correlated with Log P (0.518), Log α (0.690) and Log MW (0.676). Log α correlated with Log D (0.690), Log PSA (0.685) and Log MW (0.958). Log MW correlated with Log D (0.676) and Log α (0.958). Q, which is fixed for all compounds in a given class, did not correlate with any parameters except for Log P (-0.535). Log PSA correlated with Log P (-0.634), Log α (0.685), and Log MW (0.741). The correlation matrix for the combined data set showed that Log D correlated better with mitochondrial uptake in both the absence (0.804) and presence of

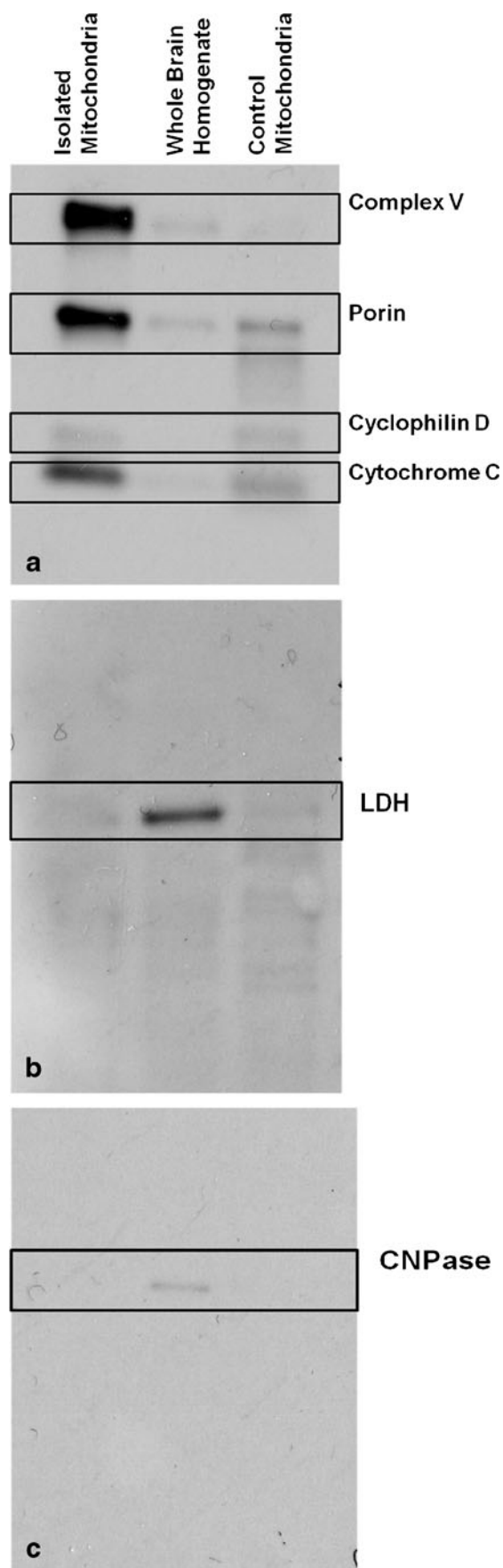


Fig. 1 Western blot of isolated brain mitochondria. **(a)** Mitochondrial proteins (complex V, porin, cyclophilin D and cytochrome c) and two contaminant proteins, **(b)** LDH (cytosolic protein) and **(c)** CNPase (myelin protein), were blotted using MitoProfile antibody cocktail, LDH antibody and CNPase antibody.

valinomycin (0.750) compared to Log P (0.565 and 0.529, respectively). Amongst the other parameters, Log D correlated the best with Log % Uptake ($R^2=0.804$), followed by Log α ($R^2=0.514$) in the absence of valinomycin. However, the only parameter that correlated significantly with the differential mitochondrial uptake was Q (0.473).

Using linear regression analysis for one parameter at a time, Log D was found to be the most significant parameter in percent uptake with strong membrane potential ($R^2=0.646$; $p<0.001$) (Table III). Charge ($R^2=0.001$; $p=0.906$), Log α ($R^2=0.264$; $p=0.02$), Log PSA ($R^2=0.003$; $p=0.825$) and Log MW ($R^2=0.179$; $p=0.063$) did not significantly contribute to Log % uptake as single parameters. Using enter method of three parameter regression analysis, the best fit equation ($R^2=0.738$; $p<0.001$) for mitochondrial uptake with strong membrane potential included the variables Log D ($p<0.001$), Log PSA ($p=0.07$), and Q ($p=0.072$). Forward stepwise linear regression eliminated Log PSA and Q from the above equation and left Log D ($p<0.001$) as a significant parameter in the model equation ($R^2=0.646$; $p<0.001$).

Use of a training set of 16 compounds from the entire set of 20 molecules resulted in equations similar to the entire dataset (Table III). Using the enter model equation ($R^2=0.716$; $p=0.001$) with Log D, Log PSA, and Q obtained from the training set, the predicted mitochondrial uptake of the test set correlated very well with their actual uptake ($R^2=0.8834$). However, prediction of the mitochondrial uptake of the test set was slightly worse ($R^2=0.731$) using the forward stepwise linear regression equation (Log D only).

For mitochondrial uptake studies with dissipated membrane potential, amongst single parameter equations, Log D ($R^2=0.563$; $p<0.001$) correlated the best compared to Log MW ($R^2=0.248$; $p=0.026$), Log α ($R^2=0.325$; $p=0.009$), Q ($R^2=0.030$; $p=0.464$), and Log PSA ($R^2=0.004$; $p=0.796$). The best fit equation ($R^2=0.567$; $p=0.003$) for mitochondrial uptake with dissipated membrane potential by valinomycin included Log D ($p=0.001$), Q ($p=0.716$), and Log PSA ($p=0.976$) using enter method of linear regression. When forward stepwise linear regression was conducted, only Log D ($p<0.001$) remained in the equation ($R^2=0.563$; $p<0.001$). Predictability of the test set was very good for both enter ($R^2=0.8671$) and forward ($R^2=0.8405$) linear regression equations obtained from the training set.

For differential mitochondrial uptake studies, the best fit equation ($R^2=0.441$; $p=0.007$) included variables Q ($p=0.005$) and Log PSA ($p=0.02$) using forward stepwise linear regression method. In addition, Q ($R^2=0.224$; $p=0.035$) correlated the best with differential mitochondrial uptake

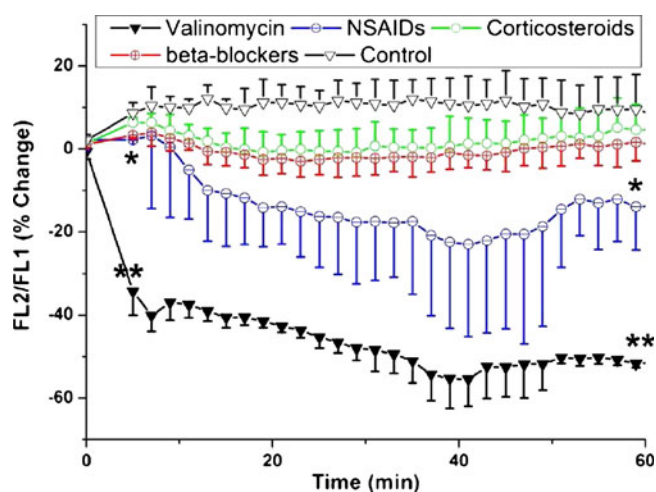


Fig. 2 The effects of valinomyacin on mitochondrial membrane potential as measured by the fluorescence emission of JC-1 dye at 590 nm (FL2) and 525 nm (FL1) following excitation at 488 nm. The arrow indicates addition of treatment (buffer, 5 μ M valinomyacin, 6.25 μ g/ml beta-blockers and NSAIDs, and 0.3125 μ g/ml corticosteroids) at 5 min. Data are presented as mean \pm SD for $n=4$. * indicates significant difference of $p < 0.05$ compared to controls. ** indicates significant difference of $p < 0.0005$ compared to controls.

compared to Log PSA ($R^2=0.093$; $p=0.192$), Log D ($R^2=0.072$; $p=0.254$), Log MW ($R^2=0.003$; $p=0.831$), and Log α ($R^2=0.0004$; $p=0.931$). Although the R^2 value for the best fit equation for differential mitochondrial uptake is relatively low compared to other data sets, the mitochondrial uptake of the test set was predicted with minimal error ($R^2=0.888$).

DISCUSSION

Isolated brain mitochondria were used in this investigation to study the influence of physiochemical properties of small molecules on mitochondrial uptake without possible confounding factors including entry across cell plasma membrane and cytosolic factors. Brain mitochondria were used as our model system for drug delivery due to the various applications in development of therapeutics for neurological disorders. The drugs chosen for this study were not primarily based on therapeutic value; however, some of these drugs may have biological roles in mediating mitochondrial function. Although NSAIDs have not yet shown a direct effect in the above disorders, specific NSAIDs including diclofenac are able to alter mitochondrial function by inducing mitochondrial swelling as a potential mechanism of side effects (18). Interestingly, propranolol (beta-blocker) also exhibits mitochondrial-specific activity by preventing cytochrome c from exiting the inner mitochondrial membrane to induce caspase activity (and apoptosis) (19), and propranolol (beta-blocker)

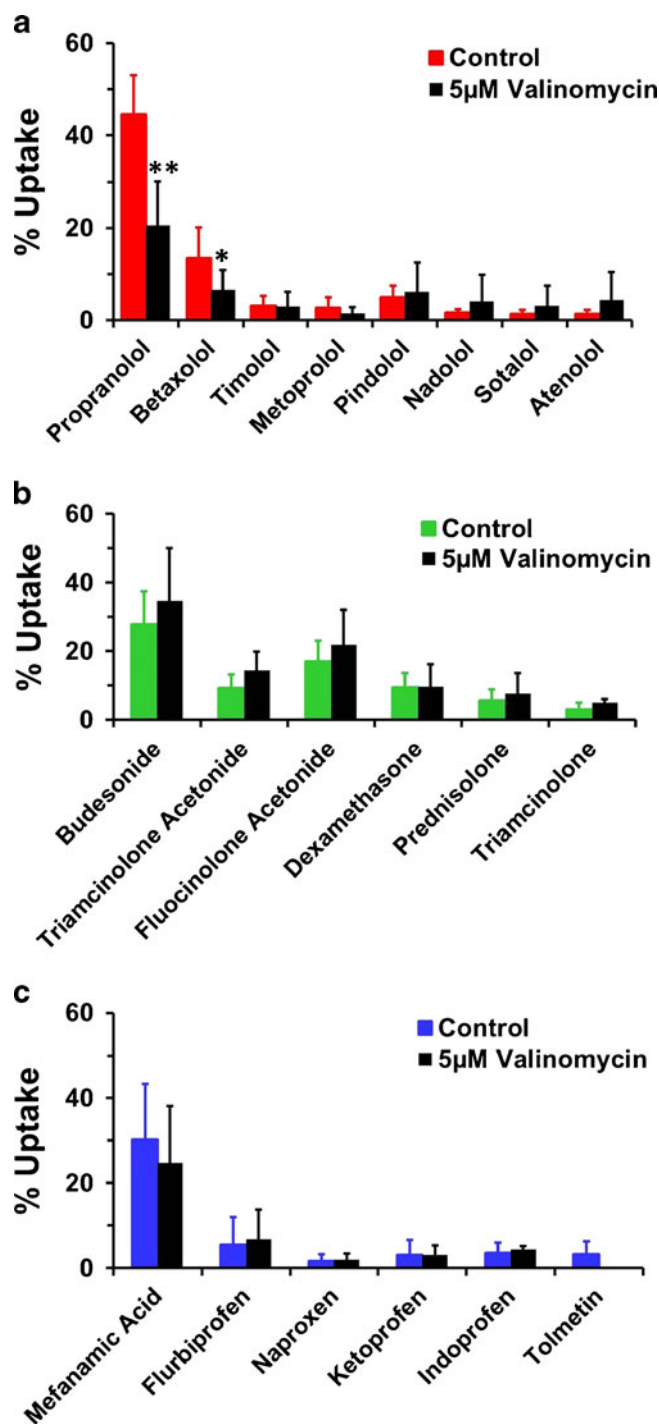


Fig. 3 Percent uptake for each drug in the absence and presence of 5 μ M valinomyacin. Drugs are listed in order of decreasing lipophilicity from left to right. Percent uptake of (a) beta-blockers, (b) corticosteroids, and (c) NSAIDs. Data are expressed as mean \pm SD, with $n=12$ for beta-blockers and corticosteroids and $n=9$ for NSAIDs. * indicates significance difference compared to controls at $p < 0.05$. ** indicates significant difference compared to controls at $p < 0.005$.

as well as metoprolol (beta-blocker) are capable of inhibiting state three mitochondrial respiration (20). Further, there is evidence that mitochondrial glucocorticoid receptor (GR)

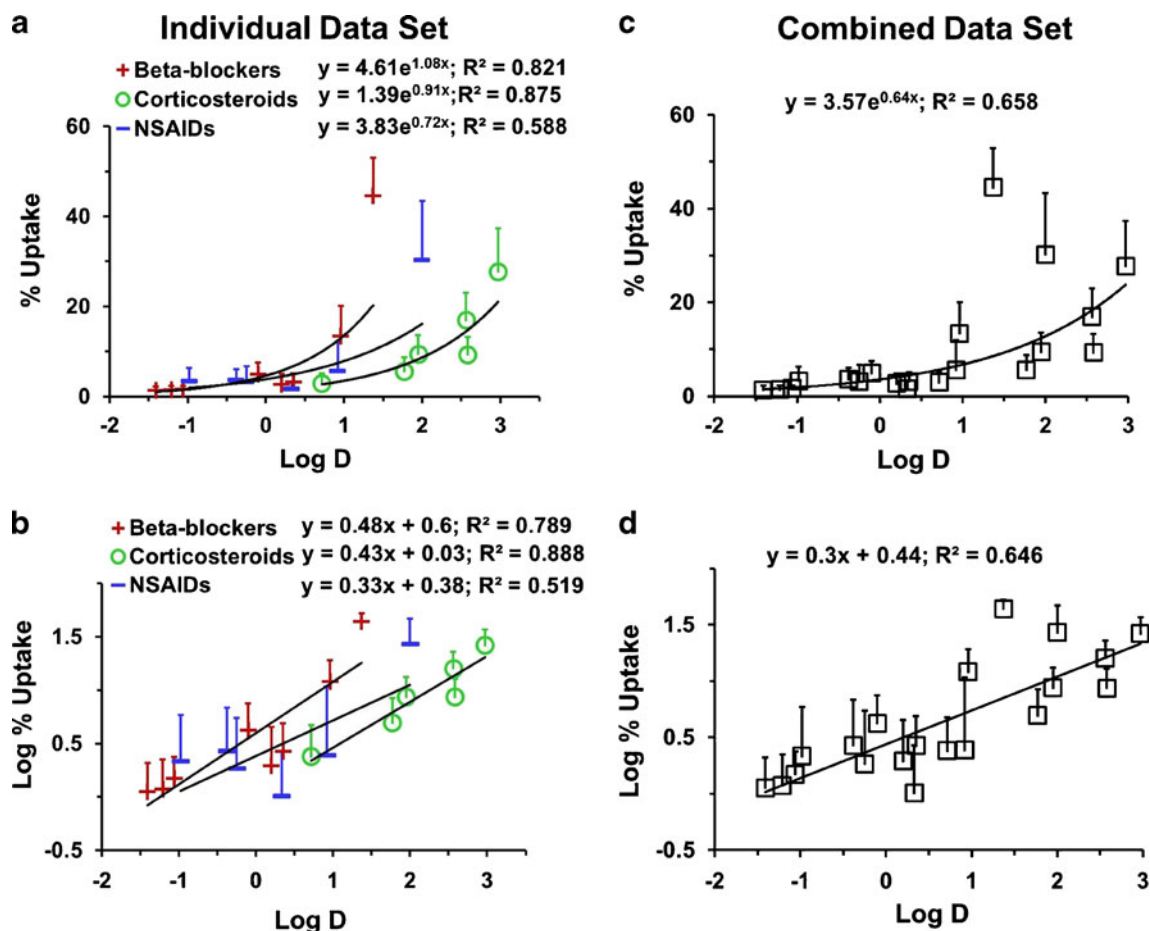


Fig. 4 Mitochondrial uptake dependency on Log D for individual data sets (**a** and **c**) and combined data set (**b** and **d**). Data are presented as mean+SD for $n = 12$ for beta-blockers and corticosteroids and $n = 9$ for NSAIDs.

is activated by dexamethasone to induce GR-mediated apoptosis (21). Drugs within each class under investigation in this study do potentially have mitochondrial actions; however, the focus of this manuscript is to investigate the influence of drug properties on their mitochondrial entry.

Our method of brain mitochondria isolation was tested for two contaminant proteins from neuronal cells as well as four mitochondria specific proteins using a western blot technique. Our isolated mitochondrial fraction was free of CNPase, a myelin protein and LDH a cytosolic protein, but

Table II Correlation Matrix of Predictor Variables in the Combined Data Set Where α Denotes Polarizability, Q Denotes Charge, and PSA is Polar Surface Area

	Log P	Log D	Log α	Log MW	Q	Log PSA	Log % Uptake	Log % Uptake with Valinomycin	Differential Log % Uptake
Log P	1	0.518 ^a	-0.081	-0.174	-0.535 ^a	-0.634 ^b	0.565 ^b	0.529 ^a	0.186
Log D	0.518 ^a	1	0.690 ^b	0.676 ^b	-0.178	0.151	0.804 ^b	0.750 ^b	0.268
Log α	-0.081	0.690 ^b	1	0.958 ^b	0.181	0.685 ^b	0.514 ^a	0.551 ^a	0.021
Log MW	-0.174	0.676 ^b	0.958 ^b	1	0.092	0.741 ^b	0.423	0.486 ^a	-0.051
Q	-0.535 ^a	-0.178	0.181	0.092	1	0.297	0.028	-0.199	0.473 ^a
Log PSA	-0.634 ^b	0.151	0.685 ^b	0.741 ^b	0.297	1	-0.053	0.087	-0.305
Log % Uptake	0.565 ^b	0.804 ^b	0.514 ^a	0.423	0.028	-0.053	1	0.899 ^b	0.407
Log % Uptake with Valinomycin	0.529 ^a	0.750 ^b	0.551 ^a	0.486 ^a	-0.199	0.087	0.899 ^b	1	-0.035
Differential Log % Uptake	0.186	0.268	0.021	-0.051	0.473 ^a	-0.305	0.407	-0.035	1

Variables with Pearson Correlation Coefficient greater than 0.5 were considered collinear.

^a indicates correlation significance at the 0.05 level and ^b indicates correlation is significant at the 0.01 level.

Table III Multiple Linear Regression Results for Mitochondrial Uptake with Strong Membrane Potential and Dissipated Membrane Potential by Valinomycin and the Differential Mitochondrial Uptake (Between With and Without Valinomycin Treatments). Enter and Forward Stepwise Methods for Linear Regression were Evaluated. Values in Parentheses Indicate Standard Error for the Estimation of the Coefficient or the Constant

Method	Best Fit Model Equation	N	R ²	Adj R ²	SE	F	P
Mitochondrial Uptake with Strong Membrane Potential							
1 All molecules, enter method	Log % Uptake = 2.032 (0.832) + 0.333 (0.05) Log D ($p=0.000005$) + 0.157 (0.081) Q ($p=0.072$) - 0.887 (0.457) Log PSA ($p=0.07$)	20	0.738	0.689	0.280	15.013	0.00005
Training set, enter method	Log % Uptake = 1.96 (1.012) + 0.344 (0.063) Log D ($p=0.0002$) + 0.174 (0.104) Q ($p=0.121$) - 0.865 (0.558) Log PSA ($p=0.147$)	16	0.716	0.645	0.313	10.090	0.001
R² for prediction of test set (betaxolol, sotalol, dexamethasone, and indoprofen) = 0.8834							
2 All molecules, forward method	Log % Uptake = 0.440 (0.077) + 0.301 (0.052) Log D ($p=0.00002$) Variables excluded by software: Q and Log PSA	20	0.646	0.626	0.307	32.828	0.00002
Training set, forward method	Log % Uptake = 0.414 (0.096) + 0.306 (0.063) Log D ($p=0.0003$)	16	0.627	0.600	0.333	23.524	0.0003
R² for prediction of test set (betaxolol, sotalol, dexamethasone, and indoprofen) = 0.731							
Mitochondrial Uptake with Dissipated Membrane Potential by Valinomycin							
3 All molecules, enter method	Log % Uptake = 0.473 (0.978) + 0.253 (0.059) Log D ($p=0.001$) - 0.035 (0.096) Q ($p=0.716$) - 0.016 (0.537) Log PSA ($p=0.976$)	20	0.567	0.486	0.330	6.993	0.003
Training set, enter method	Log % Uptake = 0.325 (1.195) + 0.267 (0.074) Log D ($p=0.004$) - 0.016 (0.123) Q ($p=0.898$) + 0.051 (0.658) Log PSA ($p=0.939$)	16	0.554	0.443	0.370	4.977	0.018
R² for prediction of test set (betaxolol, sotalol, dexamethasone, and indoprofen) = 0.8671							
4 All molecules, forward method	Log % Uptake = 0.437 (0.078) + 0.257 (0.053) Log D ($p=0.0001$) Variables excluded by software: Q and Log PSA	20	0.563	0.539	0.312	23.181	0.0001
Training set, forward method	Log % Uptake = 0.416 (0.098) + 0.270 (0.065) Log D ($p=0.001$)	16	0.554	0.522	0.343	17.373	0.001
R² for prediction of test set (betaxolol, sotalol, dexamethasone, and indoprofen) = 0.8405							
Differential Mitochondrial Uptake							
5 All molecules, forward method	Log % Uptake = 1.322 (0.508) + 0.160 (0.049) Q ($p=0.005$) - 0.711 (0.277) Log PSA ($p=0.02$) Variables excluded by software: Log D	20	0.441	0.375	0.174	6.703	0.007
Training set, forward method	Log % Uptake = 1.380 (0.579) + 0.154 (0.059) Q ($p=0.021$) - 0.745 (0.315) Log PSA ($p=0.034$)	16	0.419	0.330	0.183	4.689	0.029
R² for prediction of test set (betaxolol, sotalol, dexamethasone, and indoprofen) = 0.888							

rich in mitochondrial proteins including cytochrome c, complex V, cyclophilin D, and porin, indicating highly pure mitochondria.

The integrity of mitochondria as well as activity of valinomycin were tested using JC-1 dye and fluorescence kinetic analysis. As observed in Fig. 2, control mitochondria (buffer with JC-1 dye only) exhibited only a slight change in FL2/FL1 ratio over 1 h, which was not significant. The absolute FL2/FL1 for control mitochondria was within the range of 1.5–1.6 over 1 h (data not shown), which is indicative of a strong membrane potential of approximately -240 mV (16). Drug treatment groups had no effect on the membrane potential except for NSAIDs, which significantly reduced the potential difference by 20% at 1 h. As expected, valinomycin significantly reduced the membrane potential immediately after addition and continued to

decline over 1 h to 50%. Valinomycin is a potassium ionophore that shuttles K⁺ ions across the mitochondrial membrane (down the K⁺ concentration gradient), which results in dissipation of the membrane potential. These studies confirm that our method of isolation retains mitochondrial integrity as indicated by a substantial mitochondrial membrane potential, which can be dissipated by valinomycin exposure.

Valinomycin is commonly used to study membrane potential processes (22,23), and we chose this molecule to determine if dissipation of the membrane potential alters drug uptake of different subsets of molecules. As indicated in Fig. 3, only the % uptake of highly lipophilic, positively charged compounds (propranolol and betaxolol) was reduced in the presence of valinomycin (by 55% for propranolol and 46% for betaxolol). Therefore, the extremely

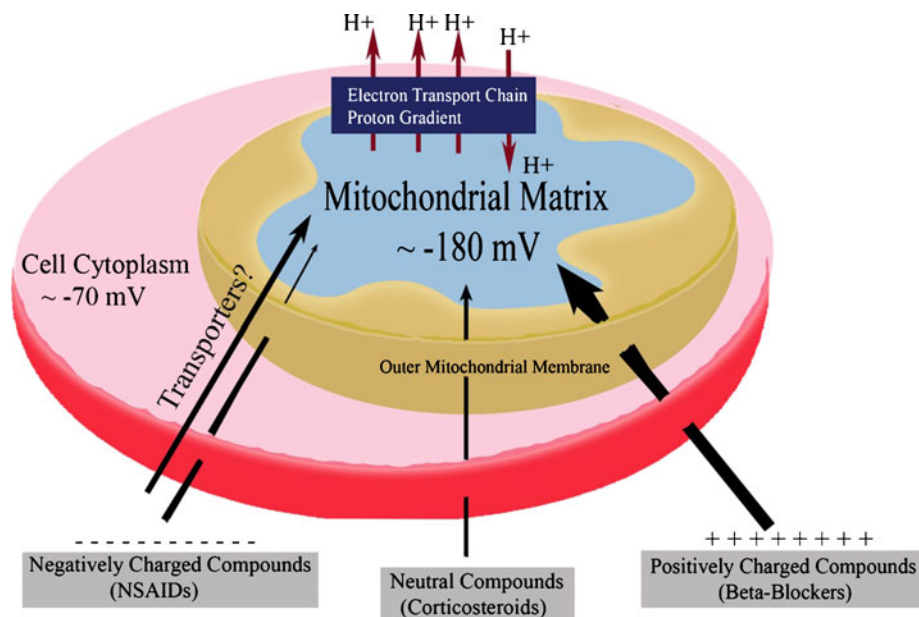
negative membrane potential may be significantly driving the uptake of these molecules. Since the % uptake of the other molecules was unaffected by dissipation in the membrane potential, their uptake might be independent of membrane potential. This is expected for neutral compounds since they carry no charge. Negatively charged compounds, on the other hand, are expected to be transported less due to high negative potential inside the mitochondria. Therefore, dissipation of the membrane potential by valinomycin was expected to reduce the energy barrier for the uptake of negatively charged compounds (Fig. 5). However, we did not observe such an enhancement in NSAID uptake following dissipation of membrane potential. Possible explanations include disruption of mitochondrial membrane potential by NSAIDs themselves and the preferential involvement of membrane transporters in the uptake of NSAIDs. We obtained evidence for the first mechanism in the fluorescence kinetic assay, where NSAIDs significantly reduced membrane potential. The second mechanism may also hold true since several anionic transporters including ABCB6, PIC, SFC1 and ANT1 are present in mitochondria. The ABCB6 (ATP-binding cassette transporter) are known to exist in the outer mitochondrial membrane (24). There also exist transporters for anionic agents necessary for mitochondrial function including, phosphate (Pi) carrier (PIC) (25), glutamate/aspartate transporter (AGC, also known as solute carrier family 1, member 3), succinate/fumarate carrier (SFC1), and peroxisomal adenine nucleotide carrier (ANT1) (26). The mitochondrial phosphate carrier (PIC) is a symporter most known for transporting anionic phosphate coupled with proton (hydrogen without electrons) transport and also less

commonly known to transport divalent anions such as sulfate, aspartate, and anionic fatty acids. It is possible that some of these anionic transporters might contribute to NSAID uptake by mitochondria.

Lipophilicity plays a major role in mitochondrial uptake of each class of molecule. All three classes of molecules exhibited similar behavior, whereby the most lipophilic molecule (propranolol, budesonide, and mefenamic acid) in each class had higher uptake compared to hydrophilic molecules (e.g., atenolol, triamcinolone, and tolmetin). In order to investigate the role of lipophilicity in more detail, the % uptake or Log % uptake was plotted *versus* Log D (Fig. 4). Plots were made for individual classes as well as the combined data set. For individual classes as well as the entire dataset, % drug uptake increased exponentially with an increase in Log D. Further, the correlation between Log % uptake and Log D was the highest for neutrally charged compounds ($R^2=0.888$). This is expected since these molecules are neutral and uptake is driven primarily by lipophilicity. Positively charged compounds also exhibited a relatively high correlation ($R^2=0.789$), but less than neutral compounds. Uptake of negatively charged compounds correlated the least with lipophilicity ($R^2=0.519$), suggesting greater contribution of other mechanisms to NSAID uptake.

The main purpose of this study was to investigate the influence of physicochemical properties on mitochondrial uptake and develop a model to predict mitochondrial uptake using the most influential physicochemical properties. Model construction was performed on the combined and individual data sets to determine which parameters contribute significantly to mitochondrial uptake. For the

Fig. 5 Proposed mechanisms of uptake of positive, neutral, and negatively charged compounds by mitochondria. It is hypothesized that entry of positively charged beta-blockers is facilitated by the high negative potential inside mitochondria, in addition to lipophilicity. Neutral corticosteroid entry into mitochondria is primarily controlled by lipophilicity. We speculate that mitochondrial entry of negatively charged NSAIDs might be facilitated by membrane transporters in addition to lipophilicity.



combined dataset, the best equation explaining 74% of the mitochondrial uptake with strong membrane potential dataset was: $\text{Log \% Uptake} = 0.333 \text{ Log D} + 0.157 \text{ Q} - 0.887 \text{ Log PSA} + 2.032$. Thus, Log D, charge, and polar surface area collectively explain the dataset the best. Lipophilicity enhancement is well known to increase drug partitioning into lipid membranes, including mitochondrial membrane. Further, it is evident from our studies with valinomycin that membrane potential does play a role in mitochondrial uptake of positively charged, highly lipophilic beta-blockers. Enhanced uptake is anticipated for positively charged molecules due to the attractive force of negative potential within the mitochondria. Each molecule in the given class carried a similar charge but varying lipophilicity. Therefore, the key differentiating feature in the uptake within each class of molecules was Log D. We speculate that while lipophilicity allows partitioning into the outer and inner membranes of mitochondria, drug molecule charge and negative potential within mitochondria further facilitate entry of positively charged drug molecules into mitochondria. PSA or polar surface area is the sum of surface areas of polar atoms such as oxygen, nitrogen, and hydrogen and this also dictates mitochondrial permeability, whereby molecules with small PSA will have higher permeability than molecules with larger PSA. A similar observation was previously made for brain uptake of drug molecules (27).

Dissipation of the mitochondrial membrane potential with valinomycin reduces the mitochondrial uptake dependency on charge (Q, $p=0.716$) and polar surface area (Log PSA, $p=0.976$) compared to mitochondrial uptake with strong membrane potential (Q, $p=0.072$ and Log PSA, $p=0.07$). This observation is consistent with the dependency of the differential mitochondrial uptake on charge ($p=0.005$) and polar surface area ($p=0.02$) ($R^2=0.441$). Thus, not Log D, but molecular charge and polar surface area contribute to the observed difference in mitochondrial delivery between mitochondria with a strong and dissipated membrane potential. Thus, the mitochondrial membrane potential may be influencing the mitochondrial uptake of charged molecules.

In an excellent review, Horbin *et al.* (9) evaluated drug properties critical for mitochondriotropics or drugs capable of accessing mitochondria. In their summary based on various literature reports employing isolated mitochondria as well as whole cell experiments, the authors characterized over 100 compounds and determined that positive, neutral, as well as negatively charged molecules can access mitochondria. Further, they determined that high drug lipophilicity or amphiphilicity are not essential tag properties for mitochondriotropics. For the first time in this study, we employed a number of positive, neutral, and negatively charged molecules in one single study employing purified isolated mitochondria. Our studies indicated that all three

classes of molecules can gain entry into the mitochondria and the extent of delivery is dependent on lipophilicity, charge, and polar surface area.

Our experiments were conducted using a cassette dosing approach to minimize animal usage and increase the throughput. However, high throughput assays are not without limitations (28). For example, if membrane transporters facilitate NSAID mitochondrial transport, competition may exist between NSAID molecules for transport, which may alter the observed mitochondrial uptake of the individual drugs within the cassette. Despite such limitations, we believe that the data presented in this study clearly indicated the influence of drug charge and lipophilicity on mitochondrial uptake for a diverse set of drug molecules.

CONCLUSION

Mitochondrial uptake of three classes of drugs with varying charge and lipophilicity were investigated using isolated brain mitochondria. Mitochondrial uptake was in the following the order: positively charged > negatively charged > neutrally charged, at a given Log D. Further, within each class of molecules, lipophilicity significantly contributed to uptake, with the most lipophilic molecule exhibiting the highest uptake. Model development and Log D correlations confirmed that lipophilicity, charge, and polar surface area are useful in predicting mitochondrial uptake, with Log D being the most critical parameter. Higher uptake of negatively charged compounds (NSAIDs) compared to neutral corticosteroids may be due to dissipation in membrane potential by NSAIDs and/or involvement of membrane transporters.

ACKNOWLEDGMENTS & DISCLOSURES

This work was supported in part by the NIH grants R01EY018940 (UBK), R01EY017533 (UBK), R01NS45748 (MP) and R01NS039587 (MP).

REFERENCES

1. Good PF, Werner P, Hsu A, Olanow CW, Perl DP. Evidence of neuronal oxidative damage in Alzheimer's disease. *Am J Pathol.* 1996;149(1):21–8.
2. Spina MB, Cohen G. Dopamine turnover and glutathione oxidation: implications for Parkinson disease. *Proc Natl Acad Sci USA.* 1989;86(4):1398–400.
3. Geromel V, Kadhom N, Cebalos-Picot I, Ouari O, Polidori A, Munnich A, *et al.* Superoxide-induced massive apoptosis in cultured skin fibroblasts harboring the neurogenic ataxia retinitis pigmentosa (NARP) mutation in the ATPase-6 gene of the mitochondrial DNA. *Hum Mol Genet.* 2001;10(11):1221–8.

4. Carmody RJ, Cotter TG. Oxidative stress induces caspase-independent retinal apoptosis *in vitro*. *Cell Death Differ.* 2000;7(3):282–91.
5. Dunaief J. Iron induced oxidative damage as a potential factor in age-related macular degeneration: the Cogan Lecture. *Invest Ophthalmol Vis Sci.* 2006;47(11):4660–4.
6. Primea TA, Blaikie FH, Evans C, Nadtochiy SM, James AM, Dahma CC, *et al.* A mitochondria-targeted S-nitrosothiol modulates respiration, nitrosates thiols, and protects against ischemia-reperfusion injury. *Proc Natl Acad Sci USA.* 2009;106(26):10764–9.
7. Zhao K, Zhao GM, Wu D, Soong Y, Birk AV, Schiller PW, *et al.* Cell-permeable peptide antioxidants targeted to inner mitochondrial membrane inhibit mitochondrial swelling, oxidative cell death, and reperfusion injury. *J Biol Chem.* 2004;279(33):34682–90.
8. Neroev V, Archipova M, Bakeeva L, Fursova A, Grigorian E, Grishanova A, *et al.* Mitochondria-targeted plastoquinone derivatives as tools to interrupt execution of the aging program. 4. Age-related eye disease. SkQ1 returns vision to blind animals. *Biochemistry (Moscow).* 2008;73(12):1317–28.
9. Horobin RW, Trapp S, Weissig V. Mitochondriotropics: a review of their mode of action, and their applications for drug and DNA delivery to mammalian mitochondria. *J Control Release.* 2007;121(3):125–36.
10. Kamo N, Muratsugu M, Hongoh R, Kobatake Y. Membrane potential of mitochondria measured with an electrode sensitive to tetraphenyl phosphonium and relationship between proton electrochemical potential and phosphorylation potential in steady state. *J Membr Biol.* 1979;49(2):105–21.
11. Kadam RS, Kompella UB. Influence of lipophilicity on drug partitioning into sclera, choroid-retinal pigment epithelium, retina, trabecular meshwork, and optic nerve. *J Pharmacol Exp Ther.* 2010;332(3):1107–20.
12. Thakur A, Kadam RS, Kompella UB. Influence of drug solubility and lipophilicity on transscleral retinal delivery of six corticosteroids. *Drug Metab Dispos.* 2010;39(5):771–81.
13. Castello PR, Drechsel DA, Patel M. Mitochondria are a major source of paraquat-induced reactive oxygen species production in the brain. *J Biol Chem.* 2007;282(19):14186–93.
14. Sims NR, Anderson MF. Isolation of mitochondria from rat brain using Percoll density gradient centrifugation. *Nat Protoc.* 2008;3(7):1228–39.
15. Drechsel DA, Patel M. Respiration-dependent H₂O₂ removal in brain mitochondria via the thioredoxin/peroxiredoxin system. *J Biol Chem.* 2010;285(36):27850–8.
16. Cossarizza A, Ceccarelli D, Masini A. Functional heterogeneity of an isolated mitochondrial population revealed by cytofluorometric analysis at the single organelle level. *Exp Cell Res.* 1996;222(1):84–94.
17. Kadam RS, Kompella UB. Cassette analysis of eight beta-blockers in bovine eye sclera, choroid-RPE, retina, and vitreous by liquid chromatography-tandem mass spectrometry. *J Chromatogr B Analyt Technol Biomed Life Sci.* 2009;877(3):253–60.
18. Lala N, Kumara J, Erdahla WE, Pfeiffera DR, Gadda ME, Graffi G, *et al.* Differential effects of non-steroidal anti-inflammatory drugs on mitochondrial dysfunction during oxidative stress. *Arch Biochem Biophys.* 2009;490(1):1–8.
19. Polster BM, Basanez G, Young M, Suzuki M, Fiskum G. Inhibition of Bax-induced cytochrome c release from neural cell and brain mitochondria by dibucaine and propranolol. *J Neurosci.* 2003;23(7):2735–43.
20. Dreisbach AW, Greif RL, Lorenzo BJ, Reidenberg MM. Lipophilic beta-blockers inhibit rat skeletal muscle mitochondrial respiration. *Pharmacology.* 1993;47(5):295–9.
21. Sionov RV, Cohen O, Kfir S, Zilberman Y, Yefenof E. Role of mitochondrial glucocorticoid receptor in glucocorticoid-induced apoptosis. *J Exp Med.* 2006;203(1):189–201.
22. Smiley ST, Reers M, Mottola-Hartshorn C, Lin M, Chen A, Smith TW, *et al.* Intracellular heterogeneity in mitochondrial membrane potentials revealed by a J-aggregate-forming lipophilic cation JC-1. *Proc Natl Acad Sci USA.* 1991;88(9):3671–5.
23. Johnson LV, Walsh ML, Bockus BJ, Chen LB. Monitoring of relative mitochondrial membrane potential in living cells by fluorescence microscopy. *J Cell Biol.* 1981;88(3):526–35.
24. Krishnamurthy PC, Du G, Fukuda Y, Sun D, Sampath J, Mercer KE, *et al.* Identification of a mammalian mitochondrial porphyrin transporter. *Nature.* 2006;443(7111):586–9.
25. Zackova M, Kramer R, Jezek P. Interaction of mitochondrial phosphate carrier with fatty acids and hydrophobic phosphate analogs. *Int J Biochem Cell Biol.* 2000;32(5):499–508.
26. Palmieri F. The mitochondrial transporter family (SLC25): physiological and pathological implications. *Pflugers Arch.* 2004;447(5):689–709.
27. Garg P, Verma J, Roy N. *In silico* modeling for blood–brain barrier permeability predictions. Springer US: *Drug Absorption Studies*; 2008. p. 510–56.
28. Smith NF, Raynaud FI, Workman P. The application of cassette dosing for pharmacokinetic screening in small-molecule cancer drug discovery. *Mol Cancer Ther.* 2007;6(2):428–40.